

BRAHMS results in the context of saturation and quantum evolution

R. Debbe¹, for the BRAHMS Collaboration

¹ Brookhaven National Laboratory,
Upton, NY 11973

Abstract. We report BRAHMS results from RHIC d+Au and p+p collisions at $\sqrt{s_{NN}} = 200\text{GeV}$. A remarkable change in the nuclear modification factor R_{dAu} is seen as the pseudorapidity of the detected charged hadrons changes from zero at mid-rapidity to 3.2 at the most forward angle studied during the 2003 run. For pseudorapidity $\eta > 1$ the suppression of the R_{cp} factor is more pronounced in the sample of central events in contrast to the behavior at mid-rapidity where the central events show higher enhancement compared to a semi-central sample. These results are consistent with a saturated Au wave function strongly affected by quantum evolution at higher values of rapidity.

Keywords: RHIC, d+Au, p+p, saturation, quantum evolution

PACS: 25.75.Dw, 13.18.Hd, 25.75.-q

1. Introduction

The first BRAHMS results from d+Au collisions at forward rapidities have generated heated discussions since they were presented in their preliminary form at the DNP meeting in Tucson AZ. At that time, the theoretical work offered two clearly differentiated views. On one side, the groups that postulate the formation of the Color Glass Condensate CGC [1] at RHIC, had results that demonstrated the presence of Cronin enhancements [2] in CGC [3, 4, 5, 6] as well as studies that included quantum evolution to describe how the nuclear modification factor would be modified as the collisions are studied at higher rapidities [7, 8] and [9]. These groups describe the d+Au collisions as coherent multiple interactions between the deuteron valence quarks and a saturated Au wave function at small values of x . As the density of gluons in the Au nuclei grows, higher order corrections to the gluon density are included within the formalism referred as quantum evolution. The net effect of these corrections is an overall reduction of the number of gluons compared to scaled p+p collisions. The effect of quantum evolution is also

present in the centrality dependence; the more central the collisions, the stronger the effect of quantum evolution making the suppression of the number of gluons more pronounced in central events.

Other groups had worked the problem based on an standard description of the Cronin enhancement as incoherent multiple scattering at the partonic level [10, 11, 12]. This description of the d+Au collisions would continue exhibiting a Cronin type enhancement close to the deuteron fragmentation region, and the strength of the enhancement would increase with the centrality of the collision.

We present here a description of the BRAHMS results [13] within the context of saturation that includes the effects of quantum evolution. We are well aware that even though our results are consistent with the descriptions offered by the theory that includes the presence of saturation in the initial state, more measurements are necessary to eliminate other explanations.

2. Experimental results

The spectra presented in this contribution were extracted from data collected with both BRAHMS spectrometers, the mid-rapidity spectrometer (MRS) and the front section of the forward spectrometer (FFS). A detailed description of the BRAHMS experimental setup can be found in [14]. The low multiplicity of charged particles in the proton+proton and d+Au collisions required an extension of the basic apparatus with a set of scintillator counters (called INEL detectors). These detectors [15] cover pseudo-rapidities in the range: $3.1 \leq |\eta| \leq 5.29$, and define a minimum biased trigger. This trigger is estimated to select $\approx 91\% \pm 3\%$ of the 2.4 barns d+Au inelastic cross section and $71\% \pm 5\%$ of the total inelastic proton-proton cross section of 41 mb. The INEL detector was also used to select events with collision vertex within ± 15 cm of the nominal collision point with a resolution of 5 cm.

The centrality of the collision was extracted from the multiplicity of the event measured within the angular region $|\eta| \leq 2.2$ with a combination of silicon and scintillator counters [16].

2.1. Spectra

Figure 1 shows the invariant yields obtained from p+p collisions (panel a) and d+Au collisions (panel b). For each system we studied particle production at 40 degrees with the MRS spectrometer and 12 and 4 degrees with the FFS spectrometer. Each distribution was obtained from several magnetic field settings and corrected for the spectrometer acceptance, tracking and trigger efficiency. No corrections were applied to the spectra for absorption or weak decays. Statistical errors are shown as vertical lines, and an overall systematic error of 15% is assigned to each point. The p+p spectra have also been corrected for trigger efficiency by $13 \pm 5\%$ to make them minimum biased with respect to the total inelastic cross section. We fitted the spectra at $\eta = 3.2$ with a power law function $\frac{C}{(1+\frac{p_T}{p_0})^n}$ and the integral of that

function over p_T^2 is compared for consistency in table 1 with UA5 results [17] for the p+p system, as well as our own multiplicity measurement for the d+Au system [15].

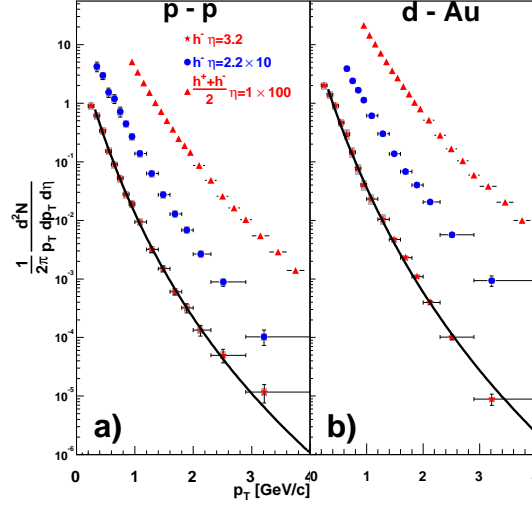


Fig. 1. Spectra for charged hadrons at different pseudo-rapidities. Panel a shows the spectra obtained from proton-proton collisions and panel b those from d+Au collisions. The top most distributions in both panels correspond to the invariant yields of $\frac{h^+ + h^-}{2}$ measured at 40 degrees with the MRS spectrometer (scaled by 100 for clarity purposes), followed by the yields of negative hadrons measured at 12 (scaled up by 10) and 4 degrees respectively. More details about these distributions can be found in Ref. [13]

System	$\frac{dN}{d\eta}_{fit}$	$\frac{dN}{d\eta}_{meas}$	Fits to power law shapes at $\eta = 3.2$		χ^2/NDF
	GeV/c				
p + p	1.05 ± 0.06	0.95 ± 0.07	1.18 ± 0.16	10.9 ± 0.9	13. / 11
d + Au	2.23 ± 0.09	2.1 ± 0.6	1.52 ± 0.1	12.3 ± 0.5	102. / 11

2.2. Nuclear modification factor R_{dAu}

The d+Au system is compared to a “simpler” one: p + p where in this particular case, we do not expect the effects of saturation. This comparison is based on the assumption that the production of moderately high transverse momentum particles

scales with the number of binary collisions N_{coll} in the initial stages. The so-called nuclear modification factor is defined as:

$$R_{dAu} \equiv \frac{1}{N_{coll}} \frac{N_{dAu}(p_T, \eta)}{N_{pp}(p_T, \eta)} \quad (1)$$

where N_{coll} is estimated to be equal to 7.2 ± 0.3 for minimum bias collisions.

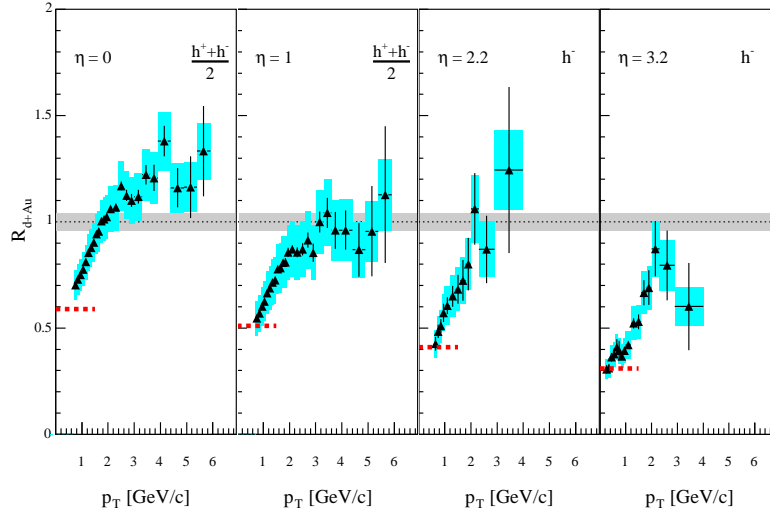


Fig. 2. Nuclear modification factor for charged hadrons at pseudorapidities $\eta = 0, 1.0, 2.2, 3.2$. Statistical errors are shown with error bars. Systematic errors are shown with shaded boxes with widths set by the bin sizes. The shaded band around unity indicates the estimated error on the normalization to $\langle N_{coll} \rangle$. Dashed lines at $p_T < 1$ GeV/c show the normalized charged particle density ratio $\frac{1}{\langle N_{coll} \rangle} \frac{dN/d\eta(d+Au)}{dN/d\eta(pp)}$.

Figure 2 shows the nuclear modification factor defined above for four η values. At mid-rapidity ($\eta = 0$), the nuclear modification factor exceeds 1 for transverse momenta greater than 2 GeV/c in a similar way as the measurements performed by Cronin at lower energies [2].

A shift of one unit of rapidity is enough to make the Cronin type enhancement disappear, and further increases in η decrease even further the nuclear modification factor R_{dAu} . Further details from this Figure 2 can be found in Ref. [13].

We see a one to one correspondence between the R_{dAu} values at low p_T and the ratio $\frac{1}{\langle N_{coll} \rangle} \frac{dN/d\eta(d+Au)}{dN/d\eta(pp)}$ as demonstrated in Fig. 2 where that ratio is shown as dashed lines at $p_T < 1$.

2.3. Centrality dependence R_{cp}

In the context of saturation, the suppression of the overall number of gluons in the Au wave function depends on a power of the number of participating nucleons N_{part}^{Au} ; the higher this number, the stronger the suppression. We extract the number of participants from the multiplicity of the collision measured in the range $|\eta| \leq 2.2$. To study the dependence on centrality or number of participants three data samples of different centralities were defined according to the multiplicity of each event, and scaled histograms in transverse momentum were filled: $N_{central}(p_T) \equiv \frac{1}{N_{coll}} N_{0-20\%}(p_T)$ for events with multiplicities ranging from 0 to 20%. $N_{semi-central}(p_T) \equiv \frac{1}{N_{coll}} N_{30-50\%}(p_T)$ for semi-central events with multiplicities ranging from 30 to 50%, and finally, $N_{periph}(p_T) \equiv \frac{1}{N_{coll}} N_{60-80\%}(p_T)$ for peripheral events with multiplicities ranging from 60 to 80% with N_{coll} values listed in table 2.

With these histograms, two ratios were constructed: $R_{CP}^{central} = \frac{N_{central}(p_T)}{N_{periph}(p_T)}$ and $R_{CP}^{semi-central} = \frac{N_{semi-central}(p_T)}{N_{periph}(p_T)}$.

Because these ratios are constructed with events from the same data run, many corrections cancel out. The only correction that was applied to these ratios is related to trigger inefficiencies that become important in peripheral events. The dominant systematic error in these ratios stems from the determination of the average number of binary collisions in each centrality data sample. This error is shown as a shaded band around 1 in Fig. 3.

Table 2. N_{part} and N_{coll} values extracted from HIJING calculations for d+Au collision

Centrality	$N_{part}(Au)$	$N_{part}(d)$	N_{coll}
Central 0 – 20%	12.5	1.96	13.6 ± 0.3
Semi – central 30 – 50%	7.36	1.79	7.9 ± 0.4
Peripheral 60 – 80%	3.16	1.39	3.3 ± 0.4

The four panels of figure 3 show the central $R_{CP}^{central}$ (filled symbols) and semi-central $R_{CP}^{semi-central}$ (open symbols) ratios for the four η settings. At $\eta = 0$ on the left-most panel, the central events yields are systematically higher than those of the semi-central events, and at the right-most panel ($\eta = 3.2$) the trend is reversed; the yields of central events are $\sim 60\%$ lower than those from semi-central events at all values of transverse momenta.

3. Discussion

Figures 2 and 3 can be described in the following way: at $\eta = 0$ the Cronin like enhancement is produced by coherent multiple scatterings of deuteron valence quarks on a saturated Au (for $x \leq 0.01$). The height of the enhancement increases with the centrality of the collisions because the number of scatterings is higher. As one

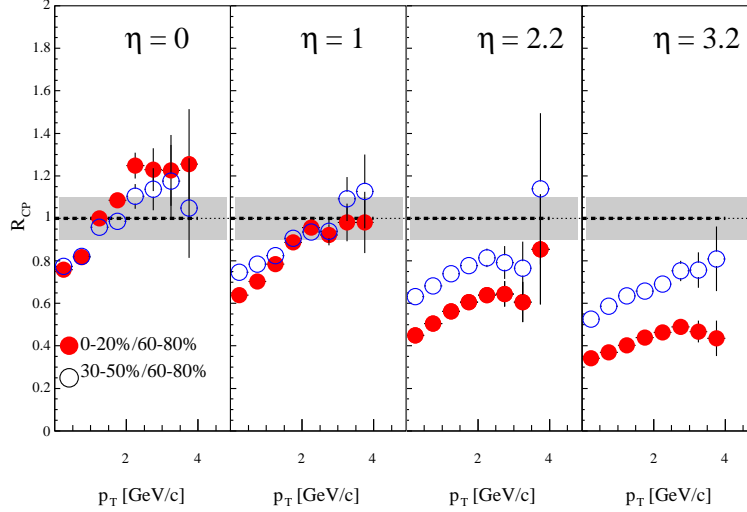


Fig. 3. Central (full points) and semi-central (open points) R_{cp} ratios (see text for details) at pseudorapidities $\eta = 0, 1.0, 2.2, 3.2$. Systematic errors ($\sim 5\%$) are smaller than the symbols. The ratios at all pseudorapidities are calculated for the average charge $\frac{h^+ + h^-}{2}$.

moves to a higher rapidity y , the probability of gluons emission grows as $P \sim \alpha_s y$ and additional corrections have to be included. These corrections can be written as: $\frac{dN}{d(\ln \frac{1}{x})} = \alpha_S(2N - N^2)$ within saturated and non-linear systems or $\frac{dN}{d(\ln \frac{1}{x})} = \alpha_S 2N$ in linear non-saturated systems. The variable N in these equations is related to the density of gluons in the nuclei. The linear term on the right side of these equations describes the emission of gluons and the quadratic term represents interactions between gluons that reduce their numbers. The numerator of the nuclear modification factor R_{dAu} is growing slowly with rapidity because of the taming effect of the quadratic term in the equation mentioned above, while the denominator continues to grow because the p+p system is more dilute. A similar suppression at all p_T is seen in Figure 2. The strength of that suppression is proportional to the number of participant nucleons in the gold ion because it implies a higher number of gluons in the system making the effect of the quadratic term more and more important. This effect is also seen in Figure 3 as the pseudorapidity of the detected particles changes from 0 to 3.2 the suppression is stronger for the central sample of events.

A recent calculation of the nuclear modification factor R_{dAu} based on a description of the Au wave function as a color glass condensate and the deuteron as a dilute system of valence quarks [18] agrees well with the BRAHMS results at $\eta = 3.2$.

Acknowledgment(s)

This work was supported by the Office of Nuclear Physics of the U.S. Department of Energy, the Danish Natural Science Research Council, the Research Council of Norway, the Polish State Committee for Scientific Research (KBN) and the Romanian Ministry of Research.

References

1. L. McLerran and R. Venugopalan, Phys. Rev. D **49**, 2233 (1994), Phys. Rev. D **49**, 3352 (1994), Phys. Rev. D **50**, 2225 (1994), Phys. Rev. D **59**, 094002 (1999); Y. V. Kovchegov, Phys. Rev. D **54**, 5463 (1996), Phys. Rev. D **55**, 5445 (1997).
2. D. Antreasyan *et al.*, Phys. Rev. D **19**, 764 (1979).
3. J. Jalilian-Marian, A. Kovner, A. Leonidov, H. Weigert, Phys. Rev. D **59**, 014014 (1999).
4. J. Jalilian-Marian *et al.* Phys. Lett. B **577**, 54-60 (2003), nucl-th/0307022.
5. A. Dumitru and J. Jalilian-Marian, Phys. Lett. B **547**, 15 (2002)
6. Yu.V. Kovchegov, Phys. Rev. D **54**, 5463 (1996).
7. D. Kharzeev, Y. V. Kovchegov and K. Tuchin Phys. Rev. D **68**, 094013, (2003), hep-ph/0307037; D. Kharzeev, E. Levin and L. McLerran, Phys. Lett. B **561**, 93 (2003).
8. D. Kharzeev, E. Levin and L. McLerran, Phys. Lett. B **561**, 93 (2003).
9. R. Baier, A. Kovner and U. A. Wiedemann Phys. Rev. D **68**, 054009, (2003); J. Albacete, *et al.* hep-ph/0307179.
10. I. Vitev, Phys. Lett. B **562**, 36 (2003)
11. Xin-Nian Wang, Phys. Lett. B **565**, 116-122, (2003).
12. A. Accardi and M. Gyulassy To be published in the Proceedings of QM2004, nucl-th/0402101.
13. I. Arsene *et al.*, BRAHMS Collaboration, Submitted to Phys. Rev. Lett. nucl-exp/0403005.
14. M. Adamczyk *et al.*, BRAHMS Collaboration, Nuclear Instruments and Methods A **499** 437 (2003).
15. I. Arsene *et al.*, Submitted to Phys. Rev. Lett. nucl-ex/0401025.
16. Y.K. Lee *et al.*, Nuclear Instruments and Methods A **516** 281 (2004).
17. G. J. Alner *et al.*, Z. Phys. C **33**, 1 (1986).
18. Jamal Jalilian-Marian nucl-th/0402080.